Mol Cell Biochem (2017) 425:9–24
DOI 10.1007/s11010-016-2858-z

Oxidative stress-induced CREB upregulation promotes DNA damage repair prior to neuronal cell death protection

Nicolás Pregi[1] · Laura María Belluscio[1] · Bruno Gabriel Berardino[1] · Daniela Susana Castillo[1] · Eduardo Tomás Cánepa[1]

Received: 23 June 2016 / Accepted: 22 October 2016 / Published online: 5 November 2016

Abstract cAMP response element-binding (CREB) protein is a cellular transcription factor that mediates responses to different physiological and pathological signals. Using a model of human neuronal cells we demonstrate herein, that CREB is phosphorylated after oxidative stress induced by hydrogen peroxide. This phosphorylation is largely independent of PKA and of the canonical phosphoacceptor site at ser-133, and is accompanied by an upregulation of CREB expression at both mRNA and protein levels. In accordance with previous data, we show that CREB upregulation promotes cell survival and that its silencing results in an increment of apoptosis after oxidative stress. Interestingly, we also found that CREB promotes DNA repair after treatment with hydrogen peroxide. Using a cDNA microarray we found that CREB is responsible for the regulation of many genes involved in DNA repair and cell survival after oxidative injury. In summary, the neuroprotective effect mediated by CREB appears to follow three essential steps following oxidative injury. First, the upregulation of CREB expression that allows sufficient level of activated and phosphorylated protein is the primordial event that promotes the induction of genes of the DNA Damage Response. Then and when the DNA repair is effective, CREB induces detoxification and survival genes. This kinetics seems to be important to completely resolve oxidative-induced neuronal damages.

Keywords Genotoxic stress · CREB transcription factor · Neuronal cells · Phosphorylation · Apoptosis · DNA damage response

Abbreviations

H_2O_2	Hydrogen peroxide
DDR	DNA damage response
Aβ	Amyloid beta peptide
CREB	cAMP response element binding
ROS	Reactive oxygen species
BER	Base excision repair
CNS	Central nervous system

Introduction

The central nervous system (CNS) is extremely susceptible to oxidative stress on account of its high metabolic rate [1]. Additionally, the generation of free radicals during the processing of dead neuronal debris by macrophages adds to the pro-oxidant environment. These facts, coupled with the lack of the regenerative capacity of terminally differentiated post-mitotic cells of the CNS, make neurons a prime target for accumulation of DNA damage and, ultimately, tissue atrophy [2]. Consistently, several major neurodegenerative disorders, such as Lou Gehrig's disease, Alzheimer's disease (AD), Parkinson's

Nicolás Pregi and Laura María Belluscio have contributed equally to this work.

Electronic supplementary material The online version of this article (doi:10.1007/s11010-016-2858-z) contains supplementary material, which is available to authorized users.

✉ Nicolás Pregi
npregi@qb.fcen.uba.ar

[1] Laboratorio de Neuroepigenética, Departamento de Química Biológica, Facultad de Ciencias Exactas y Naturales, Universidad de Buenos Aires, IQuiBiCEN–CONICET (Consejo Nacional de Investigaciones Científicas y Técnicas), Ciudad Universitaria Pabellón II Piso 4, C1428EHA Buenos Aires, Argentina

disease (PD) [3], Huntington's disease, and Friedreich's ataxia, display elevated oxidative tension and are probably exacerbated by the accumulation of associated DNA damage [4].

Oxidative damage of DNA bases is a type of genomic DNA lesion that commonly results from the action of reactive oxygen species (ROS). ROS can be generated endogenously by normal cellular metabolism through electron transport 'leaks' from the inner membrane of mitochondria, or during inflammatory processes [5]. In addition, exogenously generated ROS are induced by environmental oxidative stressors such as bromate, chromate, arsenate, sunlight, and ionizing radiation [6]. Previously, we and others had already suggested that oxidative stress-induced free radical production and/or inflammatory processes also contribute to the pathogenesis in AD [7, 8]. AD is an age-related neurodegenerative disorder that is characterized by progressive loss of memory and deterioration of higher cognitive functions, with a distinctive deposition of amyloid beta (Aβ) peptide in neuritic plaques and neuronal loss in brain regions involved in learning and memory. Aβ deposition may ultimately prove fatal through extensive neuronal cell death induced by increased production of ROS- or H_2O_2-mediated cell death [9].

Hydrogen peroxide (H_2O_2) at this physiological concentration is a major ROS, which has been implicated in many neurodegenerative conditions including Parkinson's and Alzheimer's disease (AD) [10, 11].

ROS indiscriminately react with many cellular biomolecules including proteins, lipids, and DNA to produce a variety of oxidative lesions [12]. Although most ROS have a short half-life and cause damage locally, H_2O_2 has a relatively long half-life and can travel long distances, causing DNA damage at distant sites [13]. Once into cells, ROS can cause oxidative lesions by directly acting on the DNA or indirectly through lipid peroxidation or protein damage [14, 15]. Alternatively, the damaged or stressed cells may release cytokines that bind to bystander cells, inducing the local production of ROS possibly by activating transcription of NO synthase and cyclooxygenase II [15, 16]. Elevated ROS levels can lead to oxidative stress in a cell which in turn can result in permanent changes in the genome.

DNA damage response (DDR) mechanisms are essential for maintaining genomic integrity and an accurate transmission of genetic information [17]. DDR consists of an intricate signaling network in which complex DNA surveillance programs play a key role [11, 18]. After sensing the damage, the activation of checkpoint mechanisms modulates cell cycle progression, DNA repair systems, and depending on the context or type/amount of damage can trigger the death of genetically unstable cells [8]. In the human genome, oxidative base lesions can occur in gene coding, regulatory, and other regions of the DNA [19]. These lesions, if not repaired, can lead to mutations, abnormal gene transcription, and epigenetic instability, which ultimately can cause adverse effects [6]. Mammalian cells have different types of repair mechanisms that are able to cope with specific types of DNA damages. The DNA repair system known as base excision repair (BER) plays a role in repairing various types of oxidative lesions, among which alkylated DNA (in the form of 3-methyladenine, 7-methylguanosine, and 7-methyladenine) is frequently produced in mammal cells [20]. Alkylated bases are first processed by BER DNA glycosylases that hydrolyze the deoxyribose *N*-glycosidic bond removing 3-methyladenine and 7-methylguanosine from the DNA strand [21].

Transcription factors (TF) are key regulators of gene expression directly controlling central processes such as proliferation, survival, self-renewal, and invasion. CREB (cAMP response element binding) protein is a cellular TF that mediates responses to different physiological and pathological signals. CREB plays also a central role in neuronal differentiation, protection, and plasticity [22, 23]. CREB activation is dependent on its phosphorylation at the Ser-133 by PKA (also known as cAMP-dependent protein kinase) and other Ser-133 kinases [24]. In the last few years, Tibbetts et al. and Sakamoto et al. [25–28] confirmed that other sites of phosphorylation could be used, and at least twenty different kinases can act to phosphorylate fourteen different serines, that in turn promote different functional mechanisms. It has been shown that CREB activation is induced after ROS and is critical for cell survival. This protective role of CREB involves the induction of several genes as BDNF and heme-oxygenase-1, that promote neuronal survival by participating in ROS detoxification processes and by induction of anti-apoptotic genes [22, 29–31]. However, less is known about how CREB participates in DDR following genomic injury. The main aim of the present work was to explore the involvement of CREB's regulation of gene expression in the early events of the cellular response to oxidative DNA damage, and the molecular mechanisms triggered by its participation. Therefore, we decided to first study the role of CREB in the cellular response to DNA damage. Afterwards we inquiry whether CREB had the ability to improve cell survival rate after efficient DNA repair. We demonstrate herein that hydrogen peroxide as a genotoxic agent increases both CREB protein expression and its phosphorylation in SH-SY5Y cells. Also, activated CREB induces the expression of DDB1 and MPG, a sensor and an effector of DNA damage repair, respectively.

Materials and methods

Cell line, culture, and transfections

Human SH-SY5Y neuroblastoma cells (CRL-2266, American Type Culture Collection ATCC) were used for this work. SH-SY5Y cells were grown in 25 cm^2 culture bottles (Falcon BD) containing 5 ml of D-MEM:Ham F12 (Invitrogen) supplemented with 2 mM glutamine, 100 U/ml penicillin, 100 g/ml streptomycin, and 10% (v/v) fetal bovine serum (FBS) [7]. SH-SY5Y cells were differentiated by treatment with 10 μM retinoic acid (RA) during 6 days. The medium was routinely replaced every 2 days and cultures maintained at 37 °C in humidified atmosphere containing 95% air–5% CO_2. Cells were transfected using Interferin (PolyPlus) for siRNA (QiaGen) and PEI (polysciences) for plasmids, according to the manufacturer's instructions. Plasmids and siRNA were transfected at a final concentration of 100 nM and 500 nM, respectively.

Experimental design

Time-course assays were developed to determine: (a) the incubation period for genotoxic stress-induced apoptosis and DNA damage, and (b) the appropriate period of siRNA or CREB overexpression treatment to prevent this. H_2O_2 concentration was adjusted to 100 μM, similar to that observed at physiological conditions. KU55933 (10 μM), PD152440 (10 μM), PD98059 (10 μM), H89 (1 μM) (Sigma-Aldrich) were added to the medium one hour prior to the correspondent treatment and adjusted to the final concentrations specified in text and figures. The vehicle DMSO (Sigma-Aldrich) was added to every control assay. Mock transfection as well as the scrambled siRNA transfection served as controls.

Cell viability determination by MTT assay

The MTT (3-(4,5-dimethylthiazol-2-yl)-2,5-diphenyltetrazolium bromide) (Sigma-Aldrich) reduction assay modified from that of Mossman [32] was used to assess cell viability. Cells were cultured in 35 mm Petri dishes at a density of 1×10^5 cell/ml for 24 h. Then, after appropriate treatments, the culture medium was removed, and then cells were incubated for 4 h at 37 °C with MTT solution at a final concentration of 0.5 mg/ml in complete culture medium. The supernatant was then removed, and cells were rinsed once with PBS. Finally, 100 μl of 0.04 M HCl in isopropanol was added to dissolve the blue formazan product (reduced MTT), which was quantified by measuring the absorbance at 570 nm test wavelength and at 655 nm reference wavelength in a microplate reader (iMark, BioRad).

Clonogenic assay

SH-SY5Y cells were plated at the appropriate dilution in 24-well plates (aprox. 100 cells/well), and then transfected with the indicated plasmids or siRNA. 24–36 h later, cells were treated with the genotoxic agent (H_2O_2) at the indicated concentration and duration. After 10 days, colonies were detected and counted at Olympus IX71 inverted microscope with ExiAqua camera. For this, cells were fixed with 10% formaldehyde and stained with crystal violet dye (5 mg/ml in ethanol). For each combination of time and treatment, values represent: number of colony-forming units/number of colony-forming units of untreated SH-SY5Y cells [33].

Caspase 3 activity assay

After the assigned treatments, 1×10^6 cells were harvested by centrifugation at $1000 \times g$ for 5 min at 4 °C. Cell pellets were washed once with 1 ml of PBS, then suspended in 100 μl of lysis buffer (50 mM Tris–HCl pH 7.4, 1 mM EDTA, 10 mM EGTA) containing 1 mM PMSF protease inhibitor, and maintained for 60 min on ice with occasional agitation. Cell debris was removed by centrifugation at $10{,}000 \times g$ for 20 min at 4 °C. Cell lysates were then transferred to a microplate, placing 100 μl per well. Then, 10 μl of 7.8 mM Ac-DEVD-pNA (Sigma-Aldrich) were added and the volume completed to 200 μl with the reaction buffer (100 mM HEPES pH 7.5, 0.5 mM EDTA, 5 mM DTT, 20% glycerol). Plates were covered and incubated at 37 °C for 2–4 h until a yellowish color was observed. The amount of released *p*-nitroaniline was measured spectrophotometrically at 405 nm in a microplate reader (iMark, BioRad) and caspase-3 activity was estimated as absorbance at 405/μg of total protein [34].

Analysis of apoptosis by fluorescent staining of the nucleus

SH-SY5Y cells were seeded on slide cover slips plated in 24-well dishes during 48 h. Four wells per experimental condition were simultaneously run. Cells were fixed with 4% (v/v) paraformaldehyde in PBS solution for 20 min at 4 °C, stained with 0.05 g/l Hoechst 33258 (Sigma-Aldrich) dye in PBS for 20 min at room temperature, washed twice with PBS and, mounted using fluorescent mounting medium (DAKO). Fluorescent nuclei with apoptotic characteristics were detected by fluorescent microscopy under UV illumination at 365 nm (IX71, Olympus, Japan). The images were photographed by an ExiAqua (QImaging)

equipment and digitalized. Differential cell counting was performed by analyzing at least 500 cells [35].

Flow cytometry analysis of cell cycle

After appropriate treatments, cells (5×10^5 cells/ml) were harvested by centrifugation, washed twice with PBS, and fixed overnight with 70% ethanol at 4 °C. Then, cells were washed once with PBS and stained with propidium iodide (Invitrogen) (50 µg/ml) containing RNase A (Invitrogen) (200 µg/ml) at 37 °C for 60 min. The DNA content of single cells was analyzed using a FACSAria II flow cytometer (Becton–Dickinson Immunocytometry Systems, San Jose, CA, USA) and FlowJo soft.

Reporter assay for transcriptional activity

Cells were transfected as previously described [33], with minor modifications. Briefly, cells seeded in 6-well dishes were cotransfected with 2 µg 4xCRE-CAT reporter plasmid and 2 µg of pCEFL–beta-galactosidase as control expression vector. The reporter plasmid p4xCRE-CAT containing 4 CRE recognition sites cloned into pBLCAT6 reporter plasmid was already described [35]. The latter plasmid contains the beta-galactosidase gene under the control of the CEFL promoter, and was used to normalize the efficiency of individual transfections. Control transfections with carrier alone and carrier plus vector pBLCAT6 were done simultaneously in each experiment. Transfected cells were washed three times with PBS, harvested in buffer TEN (20 mM Tris–HCl, pH 8, 100 mM NaCl, 1 mM EDTA), spun for 10 min, and resuspended in 250 mM Tris–HCl, pH 7.5, 15% glycerol. Cells were lysed by three cycles of freeze-thawing. The supernatant was assayed for beta-galactosidase activity using 1 mg of *o*-nitrophenyl beta-D-galactopyranoside as substrate and measuring absorption at 420 nm. CAT activity was determined by phase extraction assay using [^{3}H]chloramphenicol and butyryl-CoA. Acetylated chloramphenicol derivatives were extracted with xylene. The organic phase was aqueous back-extracted to reduce the background, and radioactivity was quantified by scintillation counting. CAT activity was expressed as the amount of radiolabeled chloramphenicol acetylated by 1 mg of protein in 1 min and normalized for equal transfection efficiency with beta-galactosidase activity [33].

Transcriptome analysis by cDNA microarray

Briefly, HuSG9 k is a human cDNA nylon chip designed from IMAGE clones. The microarray contained 9216 spots. Among 8682 genes, 100 genes are duplicated with another clone. 434 probes served as controls. The microarray design was not enriched in specific pathways. Genes with known functions were selected when predicted genes or genes with unknown function were discarded. Probes were selected by bioinformatic analysis to match the 3′ end of the major transcripts of each gene (Microarray Quality Control (MiQC), TAGC, INSERM U928; Marseilles, France). PCR products were spotted onto nylon membranes (Hybond-$N+$, Amersham) with a MicroGrid II arrayer (Affymetrix, Santa Clara, CA, USA). PCR amplification products of selected clones were 1500 bp length on average. The robot used a print head of 16×4 arrangement of print tips. Each tip printed 144 spots in a 12×12 grid. Further details on the HuSG9 k microarray are available on the TAGC website (http://tagc.univ-mrs.fr/). Total RNA was isolated using TRIzol reagent (Invitrogen Life Technologies, Carlsbad, CA), and RNA integrity was checked on denaturing agarose gels. Reverse transcription was performed as previously described, using 2 µg of total RNA in the presence of [α-33P]dCTP [36]. A large excess of oligo(dT) primers was added during cDNA synthesis, and the labeled probe was annealed with poly(dA) to ensure the complete saturation of poly(A) tails. Hybridizations were conducted for 48 h at 68 °C in 500 µl of hybridization buffer #(Verdeil et al. 2002)#. After washing, arrays were exposed to phosphor imaging plates, which were scanned using a BAS 5000 (Fuji, Tokyo, Japan) at a 25 µm resolution. We identified biological annotation for the clusters using DAVID [37] and interaction networks using the SP_PIR_KEYWORDS as database. We applied a Bonferroni correction to account for multiple tests performed. To interpret our data, we used two functionalities in DAVID: the « Functional annotation » tool and the « Functional annotation clustering » tool. DAVID functional annotation clustering measured relationships among the annotation terms based on the share of common genes. This type of grouping of functional annotations was able to give a more insightful view of the relationships between annotation categories and terms compared with the traditional linear list of enriched terms, as highly related/redundant annotation terms may be dispersed among hundreds of other terms. Each cluster of functional annotation was associated with an enrichment score, which depended on the distribution of the enrichment (*p* values) of each member. A good enrichment score was obtained when most of the members had good *p* values. This score is a relative score instead of a statistical probability with a minimum and a maximum value. This means that enrichment scores could be considered only together, by comparing them.

Analysis of mRNA expression level by real-time RT-PCR

Total RNA was isolated by means of Trizol reagent (Invitrogen), according to manufacturers' instructions. For

qualitative analysis, electrophoresis of RNA was performed in 2% agarose gels (w/v), stained with EtBr and photographed. RNA concentration and purity were evaluated by measuring absorbance at 260 and 280 nm. An aliquot of cDNA was subjected to 35 PCR amplification cycles (94 °C for 30 s, primer annealing at 62 °C for 30 s, extension at 72 °C for 45 s) with an initial incubation at 95 °C for 5 min and a final incubation at 60 °C for 7 min for all analyzed genes. Specific primers were employed for each gene(Table I-primers list). Real-time quantitative PCR amplification of cDNA was carried out using in Opticon Real-Time DNA engine (MJ Research). The PCR efficiency for each individual sample was derived from the regression line using LinRegPCR soft. The threshold cycle number (Ct) obtained was converted into fold of relative induction using the ΔΔCt method. Values were normalized using GAPDH as a housekeeping gene. At least, three technical replicates of three independent samples were used for each experiment; a no template blank served as negative control.

Western blotting

Cell were washed with ice-cold PBS and lysed with hypotonic buffer (50 mM TRIS pH 8.0, 150 mM NaCl, 1% Triton X-100, 1 mM sodium *o*-vanadate) containing protease inhibitors (1 mMPMSF, 4 μM leupeptin, 1 μg/ml aprotinin, 2 μM pepstatin) in a ratio of 200 μl/10^7 cells. After 30 min of incubation on ice, insoluble material was removed by centrifugation (15,000×*g*, 15 min). Cell extracts were boiled for 3 min in the Laemmli sample buffer and resolved on 10% polyacrylamide-SDS gel electrophoresis. Electrophoresis under non-denaturing conditions was run in a Miniprotean III electrophoretic system (BioRad) using 10% polyacrylamide gels. After electrophoresis, protein samples were electroblotted onto nitrocellulose membrane during 1.5 h (transfer buffer: pH 8.3, 25 mM Tris, 195 mM glycine, 0.05% SDS, pH 8.3, and 20% (v/v) methanol). Membranes were blocked by 1 h incubation in Tris buffer saline (25 mM Tris, 137 mM NaCl, 3 mM KCl, pH 7.4) containing 0.1% Tween 20 and 0.5% skim-milk powder, and then incubated with appropriate concentrations of specific primary antibodies as indicated. After washing with TBS-0.1% Tween 20, the immunoblots were probed with adequate peroxidase-conjugated secondary antibody (1:1000) for 1 h at 20 °C and washed. Antigen–antibody complex signals were detected by enhanced chemiluminescence, using ECL kit and a Fujifilm Intelligent Dark Box II equipment (Fuji) coupled to a LAS-1000 digital camera. Anti-β-actin polyclonal antibody (Santa Cruz Biotech) was used to assess sample loading variations. Densitometric analysis of protein levels was performed with ImageJ software (Rasband, W.S., ImageJ, U.S. National Institutes of Health, Bethesda, Maryland, USA) (http://imagej.nih.gov/ij/) (rsb.info.nih.gov/ij/).

Phosphorylation assay

Sh-SY5Y cells were grown in 60 mm dishes and treated as indicated. Before treatment, cells were incubated with 0.5 mCi sodium orthophosphate-^{32}P for 3 h. At indicated time points, cells were washed, collected in cold PBS, and lysed in RIPA buffer. The lysates (100 μg) were incubated with the appropriate antibody (anti-total CREB) for 2 h, followed by O.N. incubation with protein AG agarose beads at 4 °C. After washing three times with RIPA buffer, samples were analyzed by immunoblotting or SDS-PAGE. Equal amounts of whole-cell extracts were subjected to immunoprecipitation with anti-CREB antibody and the immune complexes were analyzed by SDS-PAGE and autoradiography. Dried gels were exposed to a radiographic intensifying screen by Fujifilm and scanned directly using a Bio-Imaging Analyzer Fujifilm BAS-1800II.

Statistical analysis

Results are expressed as mean ± standard error (mean ± SEM). Statistical differences were assessed by analysis of variance (ANOVA) with Tukey post hoc analysis for multiple comparisons. For RT-qPCR ANOVA of two factors and Bonferroni post-test was applied. Statistical significance was set at $*p < 0.05$ and $**p < 0.01$ Data analyses were performed with PSPP soft (http://www.gnu.org/software/pspp/).

Results

Hydrogen peroxide increases CREB transcriptional activity and its phosphorylation

The transcriptional activity of CREB was investigated after treating SH-SY5Y cells with 100 μM hydrogen peroxide (H_2O_2) established by concentration curve assay, and known to produce oxidative stress and consequently single-strand breaks. For this purpose, we used a reporter gene system. SH-SY5Y cells were cotransfected with p4xCRE-CAT, a plasmid containing 4 CREB Responding Elements drive a CAT reporter gene and pCEFL-beta-galactosidase as control and harvested 24 h post-treatment. CAT activity was normalized to beta-galactosidase activity, and the results are expressed relative to the control cells. The data represent CAT activity as the mean ± SEM of four independent experiments performed in triplicate (Fig. 1a). We

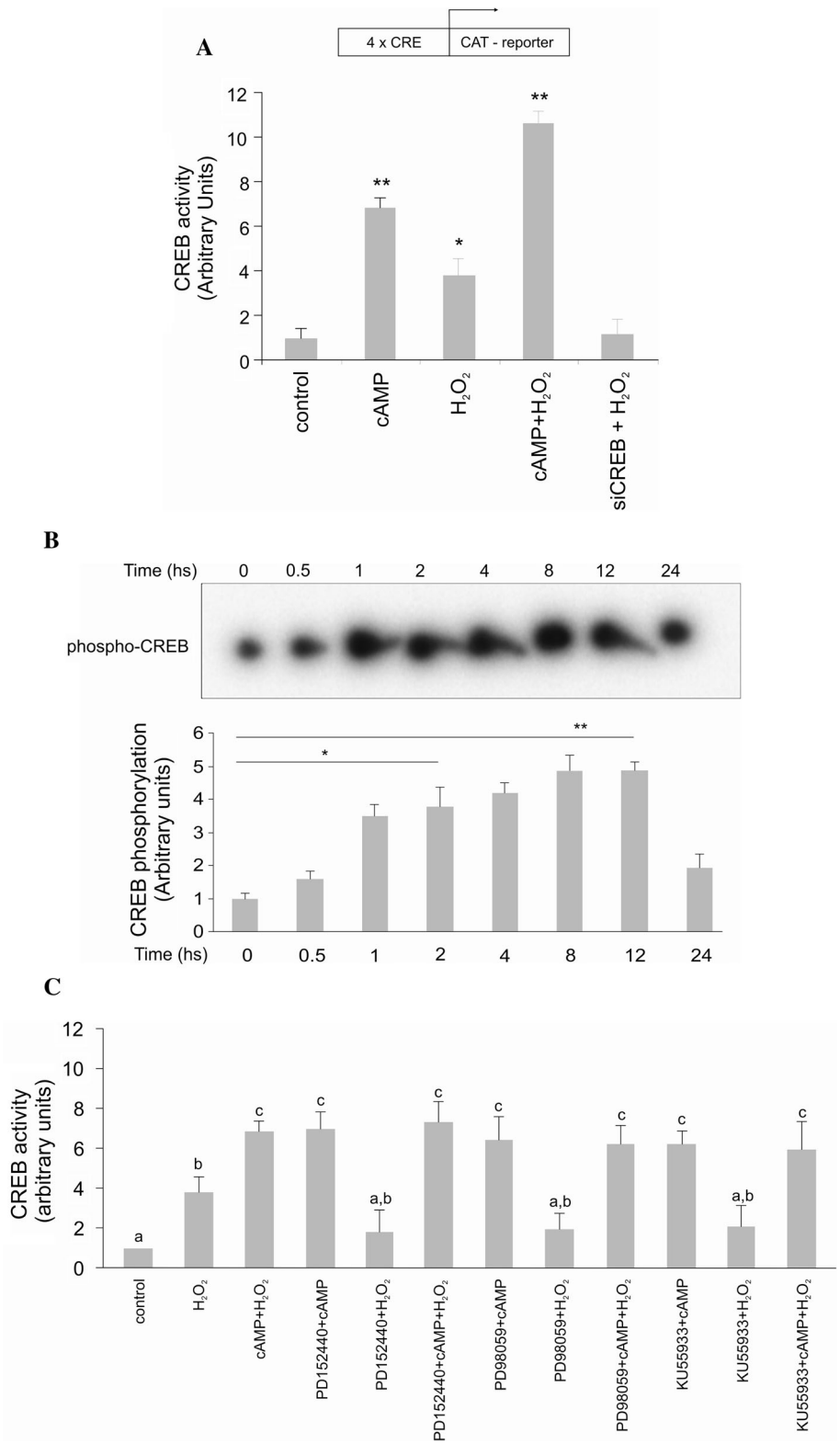

Fig. 1 Oxidative stress induces CREB activation and non-canonical phosphorylation following H_2O_2 treatment. **a** CAT reporter assay. SHSY-5Y cells were transfected with the reporter vector alone or in combination with the CREB-specific siRNA. 24 h after transfection cells were treated with 100 μM of H_2O_2 and/or 100 μM 8-CPT-cAMP or vehicle for the control condition. Cells were harvested after 12 h and processed for the CAT reporter assay. **b** SHSY-5Y cells were incubated for 24 h with normal growth medium containing 500 μCi of ^{32}P. Afterwards, 100 μM of H_2O_2 was added to the medium and cells were harvested at the indicated times for CREB phosphorylation assessment. **c** Cells were pre-treated with the indicated inhibitor for 1 h before H_2O_2 or 8-CPT-cAMP (100 μM) addition. After 24 h cells were harvested and processed for CAT reporter assay. Data represent the mean ± SEM of at least five independent experiments for (**a**) and $n = 3$ for (**b** and **c**). p values were obtained using one-way ANOVA with Tukey's post-test $*p < 0.05$, $**p < 0.01$

observed a strong increment in CREB transcriptional activity after treatment with cAMP (100 μM for 12 h), a canonical inductor of CREB, and a lower but significant induction after treatment with H_2O_2 (100 μM for 12 h). Moreover, simultaneous treatment with H_2O_2 and cAMP, with this maximally effective concentrations, revealed a synergic effect at this effective concentrations, suggesting different mechanisms of activation (Fig. 1a). Furthermore,

H_2O_2 induction is strictly CREB dependent since silencing of CREB was enough to inhibit CAT activity.

More than a decade ago, Montminy and collaborators showed that CREB's efficiency as a transcription factor is regulated by its phosphorylation [38]. In line with this, total CREB phosphorylation was induced between 1 and 12 h after treatment with H_2O_2, decreasing only after 24 h. These results show a temporal correlation between CREB activation and its total phosphorylation (Fig. 1b).

CREB contains several phosphoacceptor sites including (SQ/TQ) motifs, potentially implying several signal transduction pathways in its phosphorylation. In order to investigate which pathways are involved in CREB transcriptional activation, SH-SY5Y cells were treated with specific inhibitors before exposure to H_2O_2, and/or cAMP (Fig. 1c). Treatment of cells with an Ras farnesylation inhibitor (PD152440), an MEK1/2 inhibitor (PD98059), or an ATM competitive inhibitor (KU55933) before H_2O_2 addition, resulted in a reduction of CREB activity evidenced as a lose of significant difference with the control condition. This inhibition was no longer evident when cAMP or cAMP + H_2O_2 were used instead of H_2O_2 only. Suggesting once more the existence of an independent signal transduction pathway (most likely PKA) when cAMP is added to the medium.

Oxidative stress induces CREB expression and phosphorylation at a non-canonical site

Next, we explored whether CREB canonical phosphorylation at Ser-133 [24, 39] was induced after 6 h of treatment with H_2O_2, using a commercially available specific antibody. A 6 h incubation period was chosen based on Fig. 1b, as 4–8 h were sufficient to reach CREB maximum level of phosphorylation. As expected, CREB phosphorylation in Ser-133 was strongly induced after treatment with cAMP (Fig. 2a) and this induction was blocked by H89 (a PKA inhibitor) administration. Treatment with H_2O_2 did not yield an appreciable phosphorylation at this site, suggesting that other sites may be actively used after oxidative stress as also shown in various cell systems [26, 27]. A more detailed time-course analysis of Ser-133 phosphorylation revealed a 1.47 ± 0.12-fold increment after 12 h of H_2O_2 administration, that was accompanied by a similar increment in protein expression (1.40 ± 0.10-fold) (Fig. 2b). To assess if this upregulation occurs at the transcriptional level, we examined the expression of CREB mRNA at various time points after oxidative stress. We first observed that H_2O_2 treatment alone during 12 h is sufficient to induce a significant increase in CREBs mRNA level. The same result was also achieved by transfecting cells with a plasmid containing a functional version of CREB, not recognized by the primers designed for endogenous mRNA detection (Fig. 2c) [35]. This is consistent with previous reports showing that CREB is able to positively regulate its own transcription. On the other hand, simultaneous treatment (CREB + H_2O_2) showed a similar level of induction when compared to CREB overexpression alone, and a slightly higher (but significative) induction than H_2O_2 alone. These results suggest that there is a high but not complete, level of overlap between both mechanisms of transcriptional induction. Overall, oxidative injury induced an increment in CREBs transcriptional activation that could be mediated by an increment in its expression and/or in its phosphorylation at a non-canonical site/s.

CREB protects against oxidative stress-induced neuronal cell death

CREB is an essential transcription factor known to promote neuronal differentiation and survival [22]. In order to investigate the resulting viability and proliferation properties of neuronal cells after treatment with hydrogen peroxide, we performed both MTT and clonogenic assays. As expected, treatment with H_2O_2 diminished cell survival rate and proliferation (Fig. 3a,b H_2O_2). When cells were transfected with pCREB before oxidative stress, there was a 50% increment in cell survival rate and a reduction in oxidative stress-induced death (Fig. 3a,b CREB + H_2O_2), evidencing a cytoprotective role of CREB after oxidative stress. On the other hand, overexpression of CREB or downregulation by interference (siCREB) in the absence of oxidative stress, had no impact on the proliferation index (Fig. 3b). CREB downregulation prior to oxidative stress provoked a small but not significant decline in cell survival (Fig. 3a) when compared to H_2O_2 alone. The lack of significancy could be due to a high level of oxidative stress that hinders the detection of further cell death by this method after CREB silencing. Overall, our results point to a cytoprotective role of CREB when cells are subjected to oxidative stress.

Anti-apoptotic effect of CREB after cell cycle arrest due to hydrogen peroxide injury

To gain a better understanding of the mechanisms that promote SH-SY5Y cell survival mediated by CREB activation, we decided to analyze the effect of oxidative stress on cell cycle after pCREB transfection, and its subsequent participation in cell survival and proliferation. CREB was already shown to promote cell survival after cytotoxic stimuli via the transcriptional upregulation of neurotrophins and anti-apoptotic genes [22, 29, 31]. We therefore investigated whether CREB regulation affected cell cycle and survival after oxidative damage. Cell cytometry analysis with propidium iodide was performed

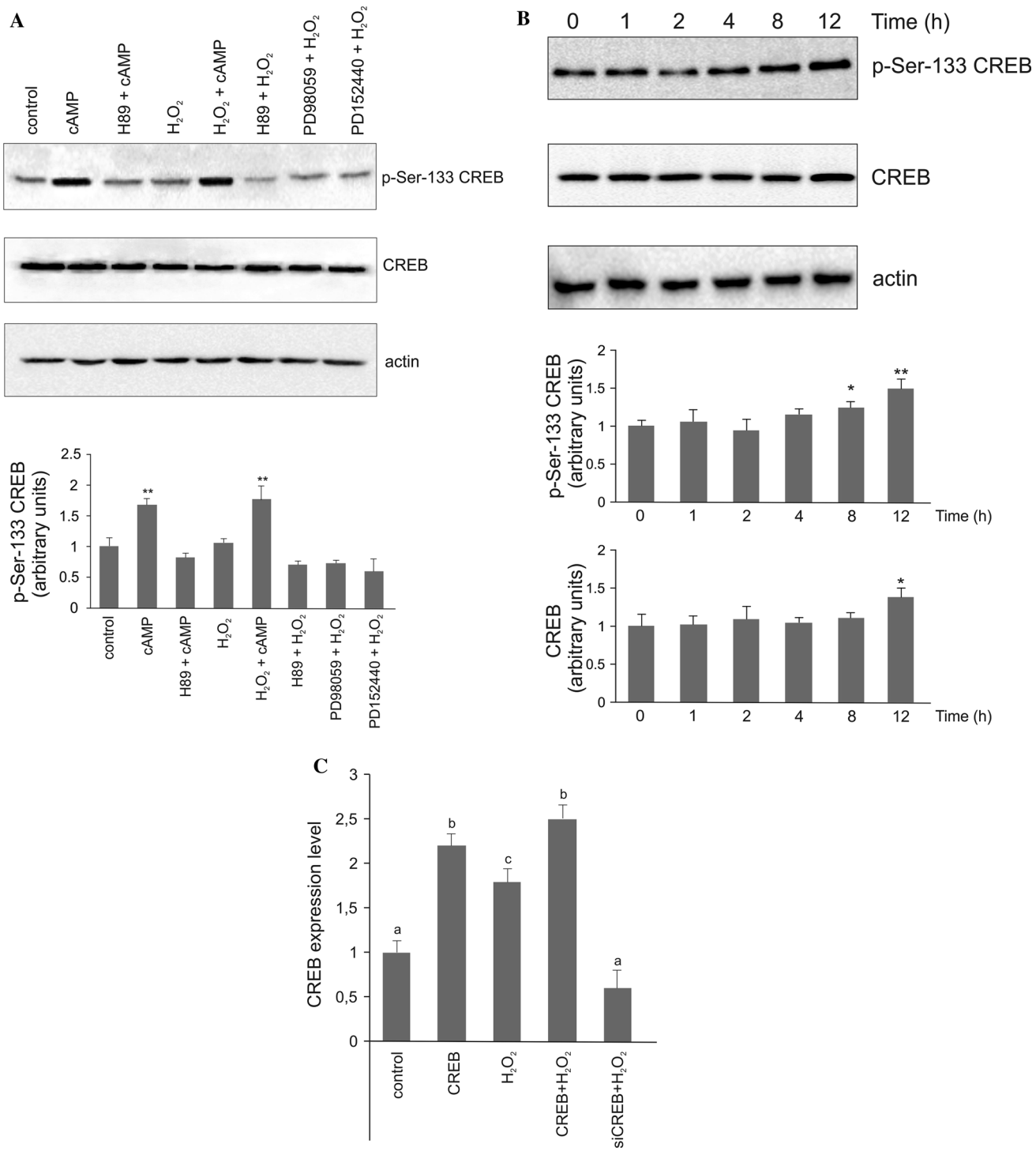

Fig. 2 H_2O_2 treatment induced CREB expression but not its phosphorylation at the canonical site (ser-133) **a** Cells were pre-treated with the indicated inhibitors for 1 h before H_2O_2 and/or cAMP addition. After 12 h cells were harvested, processed for western blot and p-ser-133-CREB, total CREB and Actin were detected using the appropriate antibodies. **b** Cells were treated with H_2O_2, harvested at the indicated times, and processed for western blot as in (a). Western blot quantification $n = 3$ per treatment. Student's t test, $^*p < 0.05$. and $^{**}p < 0.01$. pSer133CREB and total CREB quantitation normalized to actin and to the control condition. **c** CREB mRNA expression levels were assessed by RT-qPCR in cells transfected with pCREB, siCREB or mock transfected, and subsequently treated or not with H_2O_2 for 12 h. Data represent the mean ± SEM of at least three independent experiments for (**a**, **b**) and four for (**c**). p values were obtained using one-way ANOVA with Tukey's post-test for a and b and one-way ANOVA with Bonferroni's post-test for c. $^*p < 0.05$, $^{**}p < 0.01$

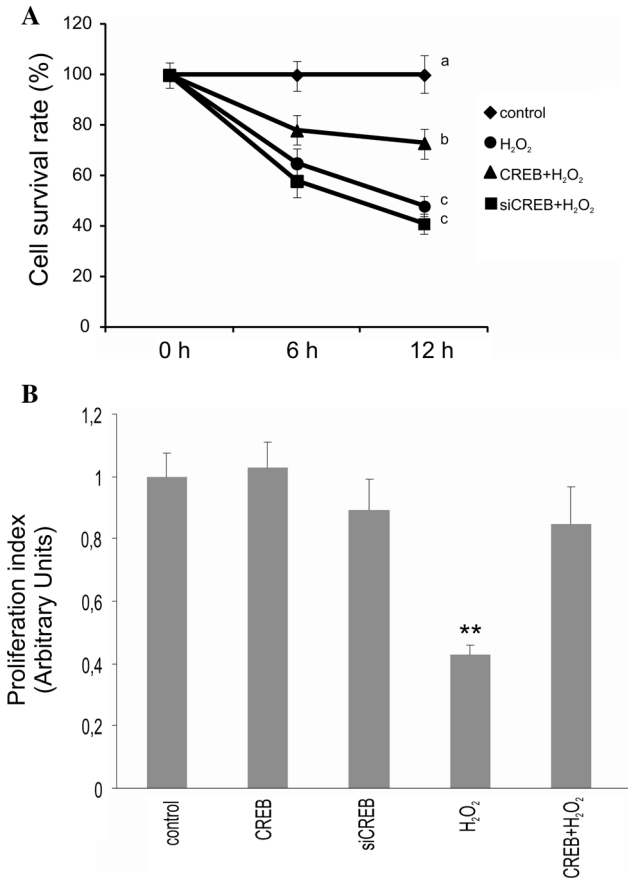

Fig. 3 CREB neuroprotective effect after H_2O_2 injury. **a** Cells were prior transfected with pCREB (100 nM) or siRNA (500 nM) and then treated or not with 100 μM of H_2O_2 for 6 or 12 h. Cell metabolism measured by the MTT assay was used to estimate cell survival. Data are representative of four independent experiments carried out in octuplicate. **b** Ten days after oxidative treatment, cell proliferation was assessed using the clonogenic assay (see Materials and methods). Data represent the mean ± SEM of four independent experiments performed in quadruplicate. Results are expressed relative to the untreated control. *p* values were calculated using one-way ANOVA $*p > 0.01$, $**p > 0.05$

on SH-SY5Y cells transfected with pCREB, siCREB, or the control vector. As shown in Fig. 4a CREB overexpression in the absence of damage had no effect on cell cycle progression. Instead, CREB silencing induced DNA fragmentation. This was evidenced as a slight increase in the number of cells in the subG1 phase of the cell cycle. When cells were treated with H_2O_2, there was a clear increment in the subG1 population (Fig. 4a, 0 h 2.91 ± 0.56, 6 h 10.28 ± 0.83, 12 h 14.32 ± 0.79). This increment was prevented by previous pCREB transfection (Fig. 4a, 6 h 4.59 ± 0.74, 12 h 4.91 ± 0.57). Treatment with H_2O_2 resulted in an increment in the proportion of cells in the S and G2/M phases at 6 h, and in G2/M at 12 h. This is consistent with the previously reported G2 arrest induced by oxidative stress.

To confirm that pCREB transfection prevented H_2O_2-induced cell death, we studied the number of apoptotic cells by Hoechst 33258 labeling (Fig. 4b) and the activation of the apoptosis pathway by caspase-3 activity (Fig. 4c). Using the same experimental design, our results show that H_2O_2 promotes a significant induction of both apoptosis and caspase-3 activity, when compared with control conditions: 13.1% ± 2.0 versus 5.7 ± 1.1% of apoptotic cells at 12 h post-treatment (Fig. 4b) or 0.41 ± 0.06 versus 0.24 ± 0.05% of caspase-3 activity at 24 h post-treatment (Fig. 4c), respectively. As expected, CREB overexpression was sufficient to protect cells from the action of the pro-apoptotic agent, since the induction of apoptosis and caspase-3 activity were both significantly reversed by transfection of pCREB prior treatment with H_2O_2 (Fig. 4c; H_2O_2 vs. CREB + H_2O_2, 12 h). Surprisingly, silencing of CREB by specific siRNA transfection 2 days prior H_2O_2 injury enhanced oxidative stress-induced apoptosis, measured both as number of cells and caspase-3 activity. These results and those of other groups [31] indicate that endogenous CREB is important for prevention of oxidative stress-induced apoptosis.

CREB induces DNA damage response mechanisms after H_2O_2

The ability of the cell cycle machinery to sense cellular injury is fundamental for genomic integrity maintenance. Checkpoint activation in response to the detection of DNA damage leads to the arrest or retardation of cell cycle progression at the corresponding phase (G1, S, G2, or M). This gives the DNA repair machinery time to exert its function, avoiding the establishment of mutations or aberrant cell replication. When the damage is too great or the repair is inefficient, activation of the cell death pathway avoids passing on fatal errors in DNA to subsequent daughter cells [40]. In this context, we decided to test whether CREB participates in the neuronal cell response to DNA damage and in the maintenance of genomic stability. Phosphorylation of histone H2AX on serine 139 (γH2AX) is a well-known indicator of genomic injury and its decrement after an appropriate time following DNA damage is an useful marker of efficient DDR. We first assessed the amount of DNA damage by measuring the levels and intensity of γH2AX foci in SH-SY5Y cells treated with hydrogen peroxide. γH2AX intensity measurements and foci number determinations were performed with CellProfiler cell image analysis software. As observed in Fig. 5a, the level of γH2AX foci increases 6 h after oxidative stress, regardless of previous CREB overexpression or silencing. At later times (12 h post-injury), the number of the γH2AX foci decreases, reaching the same level as found in the control untreated condition in cells

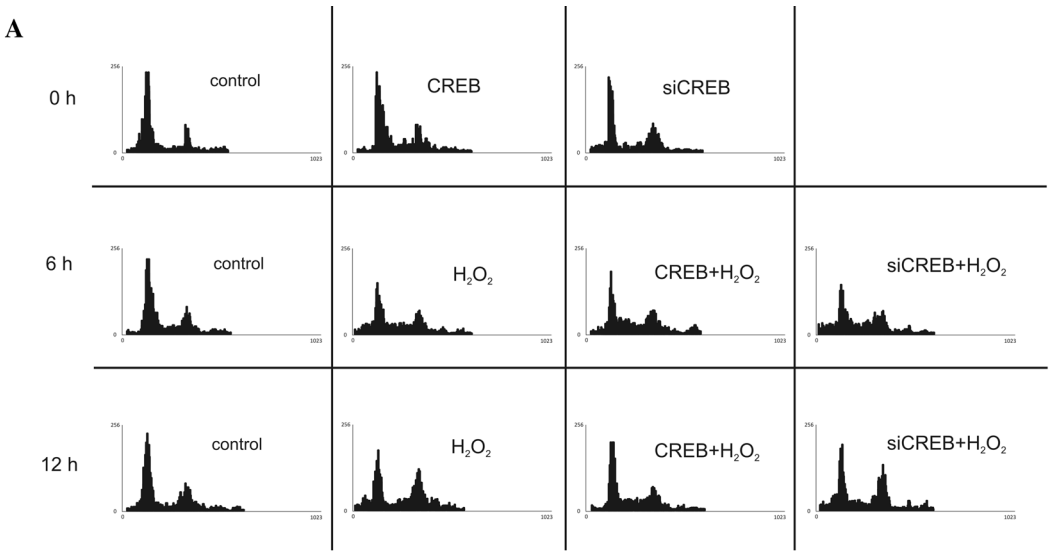

		subG1	G1	S	G2/M
0 h	control	2.91±0.56	58.34±0.65	13.73±0.46	25.12±0.81
	CREB	2.47±0.53	61.36±0.83	12.64±0.81	23.74±0.87
	siCREB	4.87±0.61	56.59±0.46	11.48±0.70	27.33±0.67
6 h	control	2.54±0.66	57.48±0.74	14.38±0.66	25.83±0.78
	H_2O_2	10.28±0.83	33.57±0.33	25.60±0.83	30.78±0.52
	CREB+H_2O_2	4.59±0.74	29.63±0.57	30.72±0.39	35.23±0.93
	siCREB+H_2O_2	12.95±0.87	30.24±0.83	27.81±0.94	29.13±0.84
12 h	control	3.27±0.65	56.38±0.54	12.75±0.86	27.85±0.74
	H_2O_2	14.32±0.79	37.71±0.69	12.73±0.55	35.39±0.59
	CREB+H_2O_2	4.91±0.57	47.71±0.91	16.89±0.61	30.61±0.93
	siCREB+H_2O_2	9.86±0.73	40.47±0.49	12.12±0.35	37.76±0.68

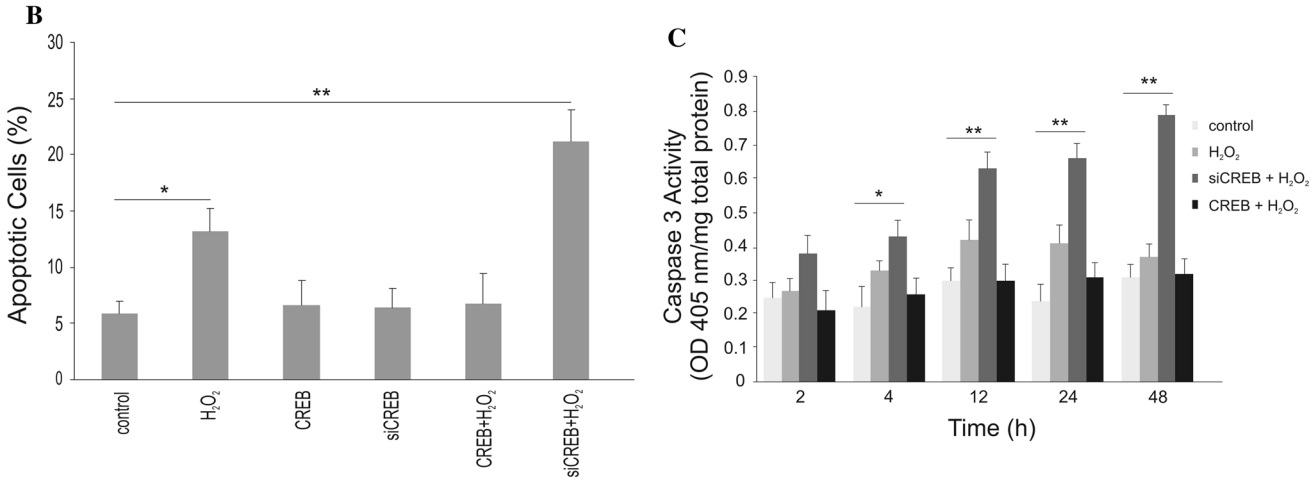

Fig. 4 CREB upregulation and activation protect cells from H_2O_2-induced cell death after treatment with H_2O_2 (100 μM; 12 h) in different conditions as indicated. **a** Cells were transfected with pCREB, siCREB, or mock transfected and incubated with H_2O_2 100 μM. At the indicated times cells were harvested, fixated, and DNA content was measured by propidium iodide staining on flow cytometry. Cyflogic and FlowJo softwares were used to plot histograms (above), gate cells, and to define the SubG1, S, G1, G2/M populations (percents shown below). **b** Cells were treated as in (**a**), fixed 6 h after H_2O_2 addition and apoptosis was analyzed by HOECHST staining. **c** caspase-3 activation was measured in cells transfected as above and treated or not with 100 μM H_2O_2 for the indicated times. *p* values were calculated using one-way ANOVA with Tukey's post-test. *$p > 0.01$; **$p > 0.05$

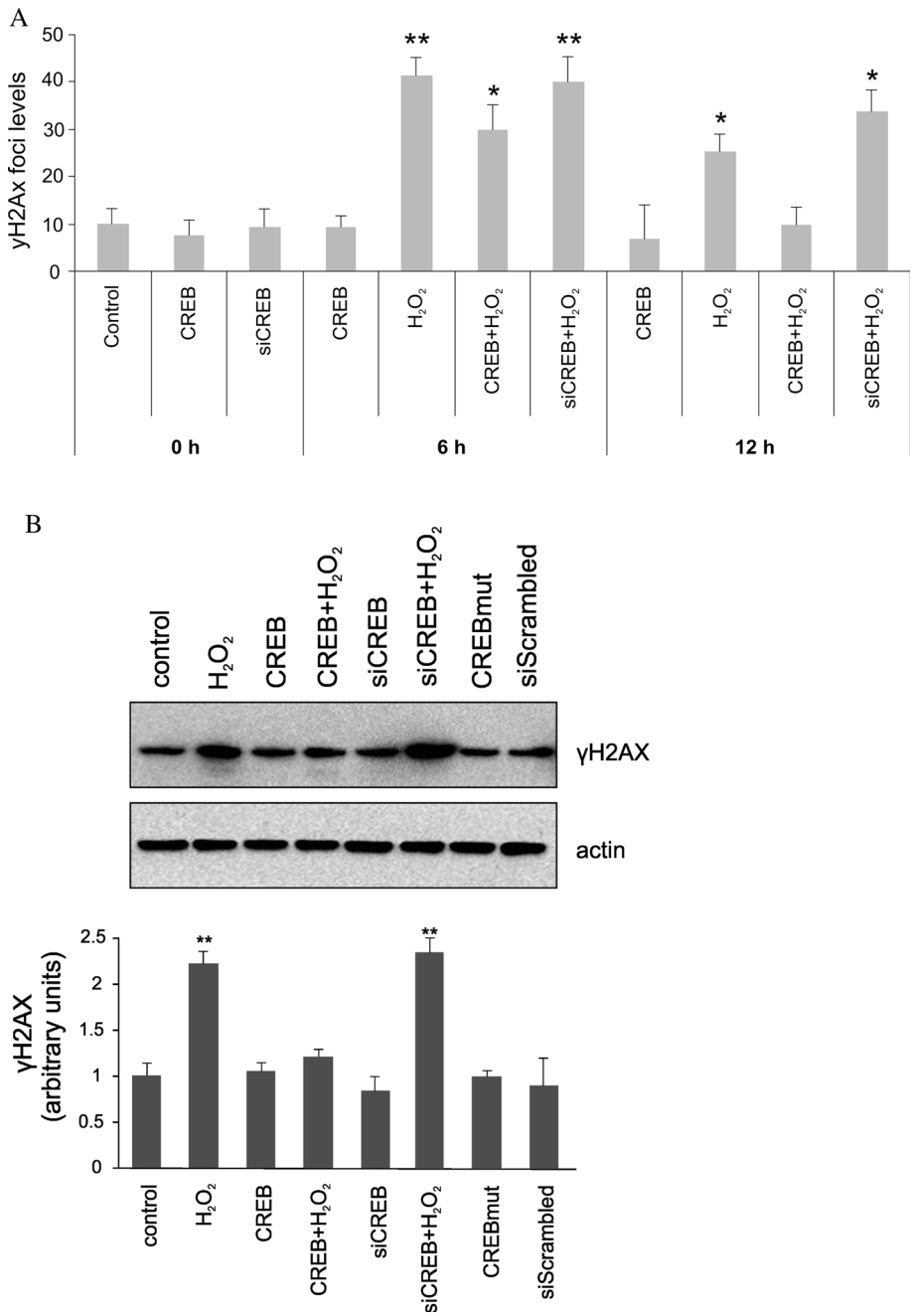

Fig. 5 CREB upregulation and activation following oxidative injury promote DNA damage repair. **a** Cells were transfected as indicated in the figure and treated with H_2O_2 100 μM for the indicated times. Immunofluorescence analysis of γH2AX foci as a marker of oxidative DNA was performed as described in materials and methods. **b** Western blot analysis of the level of γH2AX in cells treated as before. Western blot quantification $n = 3$ per treatment. Student's t test, $^{**}p < 0.01$. Data represent the mean ± SEM of three independent experiments performed in triplicate. p values were calculated using one-way ANOVA with Tukey's post-test $^{*}p > 0.01$; $^{**}p > 0.05$

that were previously transfected with pCREB. There was a tendency of cells previously transfected with siCREB to maintain higher levels of γH2AX even 12 h after genotoxic injury. γH2AX phosphorylation was also measured by western blot under the same conditions, 6 h after H_2O_2 treatment. Once again γH2AX levels increased after genotoxic insult, and this increment was efficiently reversed when cells overexpressed CREB. These results suggest that the overexpression of CREB acts on cell survival via DDR-promoting mechanisms. To our knowledge, this is the first time that CREB is implied in DDR after H_2O_2 in a neuronal system. Moreover, our results indicate that DNA repair would be resolved before cell cycle reactivation (see timing for DNA repair in Fig. 5a and for cell cycle progression in Fig. 4a).

CREB regulates the expression of DNA damage response genes

CREB is a transcriptional factor that allows the expression of a plethora of genes involved in detoxification, anti-apoptosis, and other survival processes. To see whether

CREB is also implicated in activating DNA Damage Response (DDR) genes, we analyzed the transcriptome of neuronal cells treated or not with hydrogen peroxide (12 h at 100 μM), by cDNA microarray. A specific knockdown of CREB was used before oxidative stress in order to study its involvement in gene regulation. The results of cDNA microarrays showed that over 500 genes are upregulated by H_2O_2 treatment with a Fold Change superior to 3, and that their expression is affected by CREB downregulation (Supplementary 1). Using DAVID Bioinformatics resources [41, 42] and SP_PIR_KEYWORDS as database, we performed a functional analysis of 463 genes including the identification of its biological function and cellular localization. 31% ($p < 0.005$) of these genes coded for nuclear proteins, 3.7% ($p = 0.02$) were related to the apoptotic pathway, and 1.9% ($p = 0.09$) related to DNA repair. We then focused our study on genes that code for nuclear proteins involved in DDR but are not related to apoptosis (Fig. 6a). We found five genes (MPG, XRCC3, APEX2, DDB1, and TTC5) that met these three criteria. The in silico analysis of their promoter regions revealed that only three of these five genes (APEX2, DDB1, and MPG) contain at least one CRE sequence (TGACGTCA), allowing CREB transcriptional induction. We verified the upregulation of these three genes by RT-qPCR in three independent experiments using SH-SY5Y cells treated or not with H_2O_2 (12 h at 100 μM) and previously transfected or not with siCREB. Our results show that only MPG and DDB1 are CREB dependent since silencing of CREB was sufficient to inhibit their expression. Moreover, only MPG and DDB1 were significantly upregulated (1.3 and 2.1, respectively) after oxidative injury when compared with untreated cells, whereas APEX2 was not (Fig. 6b). Collectively, our data show for the first time that oxidative injury causes DNA damage and promotes CREB upregulation and activation. CREB induction promotes DNA repair and cell survival, likely through the inductional transcription of genes involved in DDR pathways.

Discussion

Until recently, the principal neuroprotective signaling mechanism by which CREB regulates neuronal survival was thought to occur via upregulation of neurotrophin and anti-apoptotic gene expression [22]. On the other hand, new information about the role of CREB in these processes suggests that it is involved in cellular detoxification by regulating the expression of various genes involved in this process. In fact, data collected over the past few years have revealed a role for CREB in the regulation of ROS toxicity [43]. In accordance with this, NR4A nuclear orphan receptors, and PGC-1α as a key effector of ROS detoxifying enzyme expression, were both shown to be induced in a CREB-dependent manner to independently regulate distinct CREB-dependent neuroprotective pathways [29, 44]. In a recent paper [31], the authors transduced hippocampal neurons of newborn mice with a CREB coding adeno-associated virus, and found that the overexpression of CREB has led to the upregulation of several activity-regulated inhibitor of death (AID) genes, thus promoting neuronal survival. In accordance with this, we found that H_2O_2 treatment induces the expression, phosphorylation, and transcriptional activity of CREB. The induction of CREB also protected the cell from cytotoxic events such as oxidative stress, presumably via the induction of cell survival genes [31].

Apoptosis is a process of programmed cell death and is fundamental for the maintenance of brain homeostasis. Deregulation of apoptosis has been associated with different pathologies, including several neurodegenerative diseases. Therefore, neuroprotection has been critically involved in the investigation of therapeutic approaches that focuses upon growth factors as pharmacological agents to prevent neuronal cell apoptosis. Our results highlight for the first time that oxidative stress induces not only CREB phosphorylation but also its expression at both mRNA and protein level. This leads to an increment in CREB transcriptional activity and on the expression of its target genes that function to promote cell survival. Herein, we show that CREB expression is essential for cell survival after oxidative stress, as its silencing promoted an increment in the number of apoptotic cells. In fact, we show that the strong activation of caspase-3 when CREB was silenced by RNA interference prior oxidative stress confirms the importance of CREB signaling through upregulation of its synthesis, not only of its phosphorylation.

CREB's activation after oxidative injury follows a positive feedback loop, as activated CREB is able to regulate the transcription of its own mRNA. In fact, the overexpression of CREB by transfection of an expression vector was enough to protect cells from oxidative injury-induced apoptosis, as the caspase-3 activity detected under this condition was equal to the one observed in the untreated control. Furthermore, a significant difference in the activation of this caspase appears only 12 h after treatment with H_2O_2 compared with the same condition when CREB is previously silenced. This result shows that the upregulation of CREB transcription increases the quantity of phosphorylated CREB after treatment with H_2O_2 and initiates the transcription of several CREB-target genes. Previously, Tibbetts and collaborators had shown that the activation of CREB as a transcription factor is dependent on ATM phosphorylation in response of irradiation or oxidative stress [26]. In a more recent work the same group showed that ATM can either activate or inhibit

CREB's transcriptional activity depending on the amount of DNA damage. In this particular study, the authors used a human immortalized myelogenous leukemia cell line (K562). Herein, we confirm that the H_2O_2-induced phosphorylation does not only take place at the canonical Ser-133 site, suggesting that other sites of phosphorylation dependent of Ras/MapK and ATM pathways and independent of PKA are involved (as shown by others groups [25] see for review [23]). Tibbetts et al. showed that treatment with 100 μM of H_2O_2 induces partial phosphorylation of CREB at other sites than Ser-133 [26]. Further experiments are needed to investigate the identity of these alternative phosphoacceptor sites involved in CREB activation in response to oxidative stress in neuronal cells. We show here for the first time that at least in neuronal cells, CREB overexpression induces DDR genes that facilitate DNA repair, avoiding apoptosis when the amount of damage is manageable.

The DDR pathway is involved in DNA damage detection and repair after genotoxic injury. This pathway allows cell survival when the damage isn't too great and avoids passing on mutations to daughter cells. In 1999, a study done in human lymphocytes revealed that hydrogen peroxide induces single- and double-strand brakes in the DNA, and it was shown to be a potent mutation agent [45] and see for review [46]. The DNA Damage Response (DDR) pathways regulate both the activation of cell cycle checkpoints that arrest the cell either transiently or permanently, and of specific DNA repair pathways in response to DNA damage. It has been shown that CREB participates in cellular detoxification and DNA damage repair through upregulation of APE1 (an endonuclease fundamental for base excision repair) in rat primary cortical neurons [47]. Other repair enzymes independent of CREB, including XRCC1, POLB, and LIG3 have also been suggested to have neuroprotective roles following ischemia injury in rat models [48] or human cell cultures [2]. Surprisingly, the transcription of APE1, POLB, and LIG3 as well as XRCC1 did not appear to be regulated by CREB in our model of human neuronal cells, suggesting a diversity of action of CREB depending on the species, cell type or on the type of damage inductor. To date it is not known how CREB is able to promote these processes in humans. Thus, a goal of our study was to provide evidence that CREB induces not only anti-apoptotic or detoxification genes but also DNA repair proteins, all essential factors for cell survival after injury induced by oxidative stress. Oxidative DNA lesions can be difficult to quantitate in situ. However, they may lead to the formation of DSBs which can more easily be quantified by immunocytochemical detection of phosphorylated histone H2AX (γ-H2AX). When a DSB forms, many H2AX molecules become phosphorylated within a few minutes of break generation to form a γH2AX focus, a highly amplified response which enables the individual DSB site to be visualized in situ. Interestingly, the analysis of the kinetics of DNA repair by measuring the levels and intensity of γH2AX foci reveals that 12 h incubation with H_2O_2 is

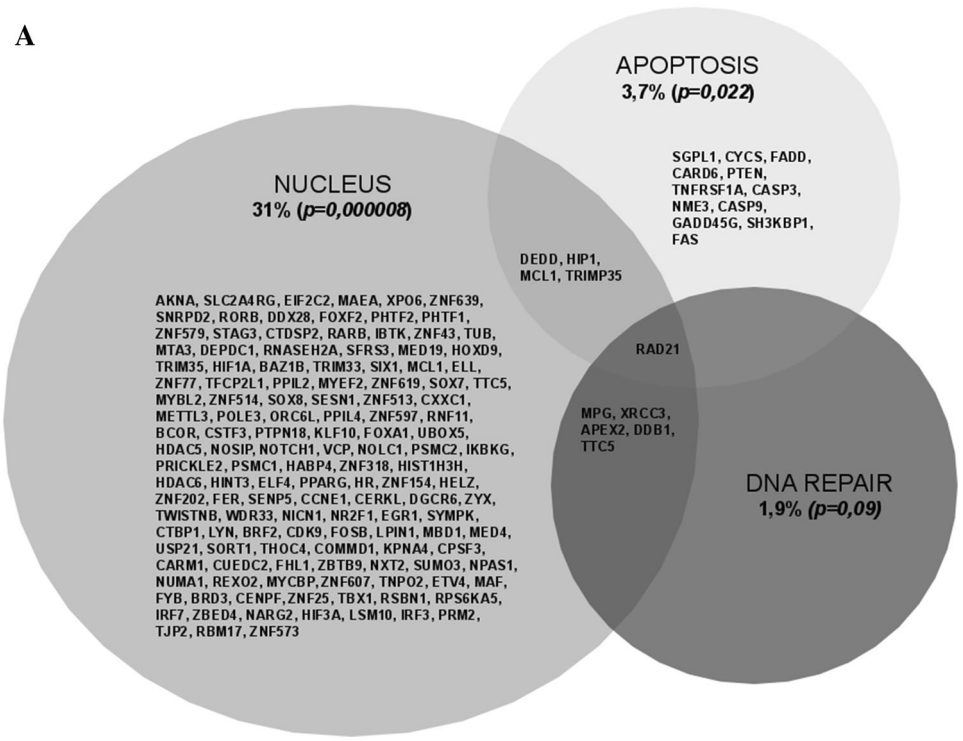

Fig. 6 CREB upregulation and activation following oxidative injury induce genes responsible for DDR mechanism. **a** Venn representation of genes induced after oxidative injury in SH-SY5Y cells, clustering for Nuclear, anti-apoptosis, or DDR proteins by DAVID functional software using the SP_PIR_KEYWORDS as database. **b** Relative mRNA expression of DDR genes after treatment with H_2O_2 (100 μM; 12 h) in different conditions as indicated. Data represent the mean ± SEM of three independent experiments. *p* values were calculated using one-way ANOVA with Tukey's post-test for a and with Bonferroni's post-test for (**b**). $*p < 0.05$, $**p < 0.01$

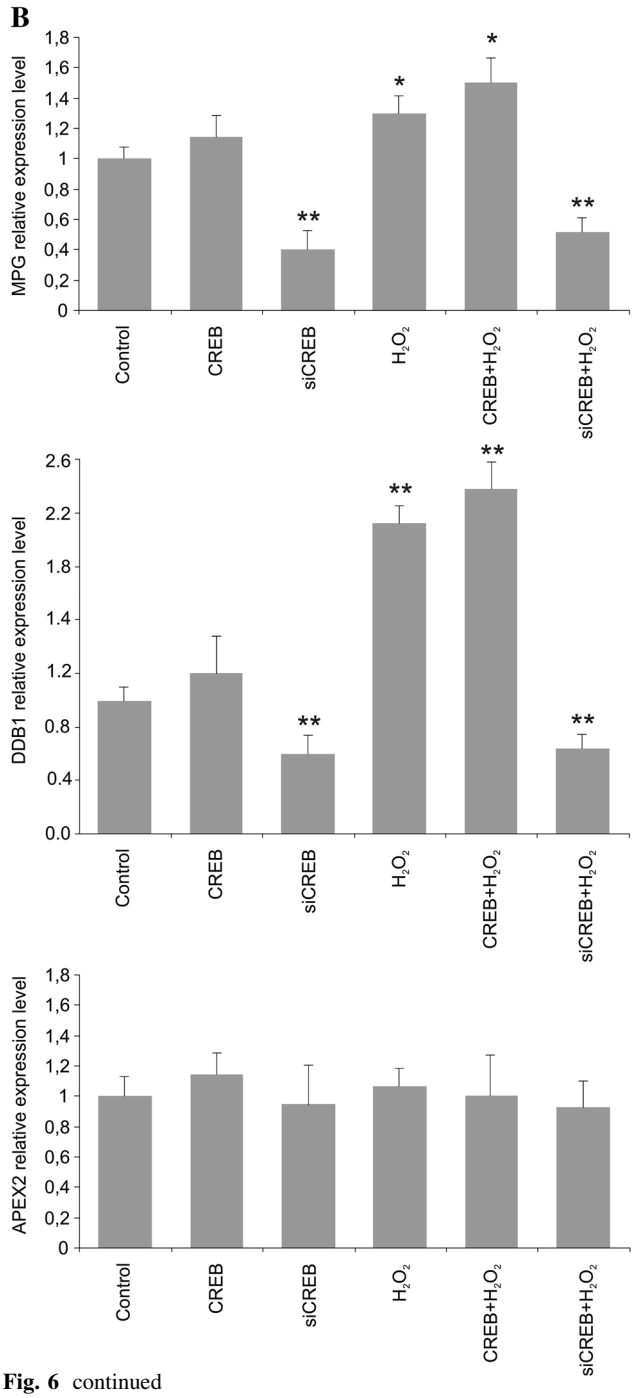

Fig. 6 continued

sufficient to promote DDR mechanisms, showing that DNA repair should be resolved before anti-apoptosis rescue illustrated by caspase-3 activity or cell cycle assays. When cells were transfected with CREB before hydrogen peroxide treatment, the amount of damage present at 12 h was indistinguishable from the control condition. We show here for the first time that CREB upregulation is involved in DNA damage repair in neuronal cells. More importantly, we demonstrate that human neuronal cells are protected from oxidative DNA damage via CREB signaling not only by inducing anti-apoptotic genes and cell cycle arrest but also the expression of genes that are responsible of DNA repair. We were also able to identify two genes whose transcription was regulated by CREB upon its activation by oxidative conditions. The presence of CRE sites in the promoters poses the possibility that its transcription could be regulated by CREB direct interaction rather than by other intermediate genes whose transcription is also dependant on CREB. Further studies of CREB interaction with their promoters can help clarify this issue. In fact, DDB1 and MPG are two proteins involved in DDR mechanism following irradiation damage, and known as respectively sensor complex of DNA damage [49] and effector of DNA repair [50]. MPG and DDB1 are both STAT3-mediated factors that were shown to be upregulated after UV-induced DNA damage [51–53]. This is the first time that they are shown to be induced also by CREB as a neuronal rescue response to oxidative DNA damage.

Finally, since several neurodegenerative diseases such as AD and PD are characterized by an upregulation of ROS and consequent oxidative stress that promotes neuronal cell death, our results could have a great impact on human health issue. Indeed, CREB signaling therapeutic could be induced to promote not only anti-apoptotic programs but also DNA repair programs to maintain genome stability in brain.

Acknowledgements This research was supported by grants from the University of Buenos Aires (UBA 2011–2013; UBA 2011-2014), the National Council of Scientific and Technical Research (CONICET, Argentina), and the National Agency for Scientific and Technologic Promotion (ANPCYT) (PICT 2012–2014; PICT 2010–2013).

References

1. Hachem LD, Mothe AJ, Tator CH (2015) Effect of BDNF and other potential survival factors in models of in vitro oxidative stress on adult spinal cord-derived neural stem/progenitor cells. Biores Open Access 4(1):146–159
2. Kulkarni A, McNeill DR, Gleichmann M et al (2008) XRCC1 protects against the lethality of induced oxidative DNA damage in nondividing neural cells. Nucleic Acids Res 36:5111–5121. doi:10.1093/nar/gkn480
3. Belaidi AA, Bush AI (2015) Iron neurochemistry in Alzheimer's disease and Parkinson's disease: targets for therapeutics. J Neurochem. doi:10.1111/jnc.13425
4. Cleary JP, Walsh DM, Hofmeister JJ et al (2005) Natural oligomers of the amyloid-beta protein specifically disrupt cognitive function. Nat Neurosci 8:79–84. doi:10.1038/nn1372
5. Leon J, Sakumi K, Castillo E et al (2016) 8-Oxoguanine accumulation in mitochondrial DNA causes mitochondrial dysfunction and impairs neuritogenesis in cultured adult mouse cortical neurons under oxidative conditions. Sci Rep 6:22086. doi:10.1038/srep22086
6. Migliore L, Coppedè F (2009) Environmental-induced oxidative stress in neurodegenerative disorders and aging. Mutat Res 674:73–84. doi:10.1016/j.mrgentox.2008.09.013

7. Pregi N, Vittori D, Pérez G et al (2006) Effect of erythropoietin on staurosporine-induced apoptosis and differentiation of SH-SY5Y neuroblastoma cells. Biochim Biophys Acta 1763:238–246
8. Bartek J, Lukas J (2007) DNA damage checkpoints: from initiation to recovery or adaptation. Curr Opin Cell Biol 19:238–245. doi:10.1016/j.ceb.2007.02.009
9. Yang S-P, Bae D-G, Kang HJ et al (2004) Co-accumulation of vascular endothelial growth factor with beta-amyloid in the brain of patients with Alzheimer's disease. Neurobiol Aging 25:283–290. doi:10.1016/S0197-4580(03)00111-8
10. Dell'Orco M, Milani P, Arrigoni L et al (2016) Hydrogen peroxide-mediated induction of SOD1 gene transcription is independent from Nrf2 in a cellular model of neurodegeneration. Biochim Biophys Acta 1859:315–323. doi:10.1016/j.bbagrm.2015.11.009
11. Jackson SP (2009) The DNA-damage response: new molecular insights and new approaches to cancer therapy. Biochem Soc Trans 37:483–494. doi:10.1042/BST0370483
12. Sedelnikova OA, Redon CE, Dickey JS et al (2010) Role of oxidatively induced DNA lesions in human pathogenesis. Mutat Res 704:152–159. doi:10.1016/j.mrrev.2009.12.005
13. Lu W, Ogasawara MA, Huang P (2007) Models of reactive oxygen species in cancer. Drug Discov Today Dis Models 4:67–73. doi:10.1016/j.ddmod.2007.10.005
14. Lala PK, Chakraborty C (2001) Role of nitric oxide in carcinogenesis and tumour progression. Lancet Oncol 2:149–156. doi:10.1016/S1470-2045(00)00256-4
15. Hussain S, Witt E, Huber PAJ et al (2003) Direct interaction of the Fanconi anaemia protein FANCG with BRCA2/FANCD1. Hum Mol Genet 12:2503–2510. doi:10.1093/hmg/ddg266
16. Tartier L, Gilchrist S, Burdak-Rothkamm S et al (2007) Cytoplasmic irradiation induces mitochondrial-dependent 53BP1 protein relocalization in irradiated and bystander cells. Cancer Res 67:5872–5879. doi:10.1158/0008-5472.CAN-07-0188
17. Kurfurstova D, Bartkova J, Vrtel R et al (2016) DNA damage signalling barrier, oxidative stress and treatment-relevant DNA repair factor alterations during progression of human prostate cancer. Mol Oncol. doi:10.1016/j.molonc.2016.02.005
18. Simoneau A, Ricard É, Weber S et al (2016) Chromosome-wide histone deacetylation by sirtuins prevents hyperactivation of DNA damage-induced signaling upon replicative stress. Nucleic Acids Res. doi:10.1093/nar/gkv1537
19. Bellacosa A, Drohat AC (2015) Role of base excision repair in maintaining the genetic and epigenetic integrity of CpG sites. DNA Rep (Amst) 32:33–42. doi:10.1016/j.dnarep.2015.04.011
20. Chou W-C, Hu L-Y, Hsiung C-N, Shen C-Y (2015) Initiation of the ATM-Chk2 DNA damage response through the base excision repair pathway. Carcinogenesis 36:832–840. doi:10.1093/carcin/bgv079
21. Maynard S, Schurman SH, Harboe C et al (2009) Base excision repair of oxidative DNA damage and association with cancer and aging. Carcinogenesis 30:2–10. doi:10.1093/carcin/bgn250
22. Lonze BE, Ginty DD (2002) Function and regulation of CREB family transcription factors in the nervous system. Neuron 35:605–623
23. Sakamoto K, Karelina K, Obrietan K (2011) CREB: a multifaceted regulator of neuronal plasticity and protection. J Neurochem 116:1–9. doi:10.1111/j.1471-4159.2010.07080.x
24. Gonzalez GA, Montminy MR (1989) Cyclic AMP stimulates somatostatin gene transcription by phosphorylation of CREB at serine 133. Cell 59:675–680
25. Gonzalez GA, Yamamoto KK, Fischer WH et al (1989) A cluster of phosphorylation sites on the cyclic AMP-regulated nuclear factor CREB predicted by its sequence. Nature 337:749–752. doi:10.1038/337749a0
26. Shi Y, Venkataraman SL, Dodson GE et al (2004) Direct regulation of CREB transcriptional activity by ATM in response to genotoxic stress. Proc Natl Acad Sci USA 101:5898–5903. doi:10.1073/pnas.0307718101
27. Sakamoto K, Huang B-W, Iwasaki K et al (2010) Regulation of genotoxic stress response by homeodomain-interacting protein kinase 2 through phosphorylation of cyclic AMP response element-binding protein at serine 271. Mol Biol Cell 21:2966–2974. doi:10.1091/mbc.E10-01-0015
28. Trinh AT, Kim SH, Chang H et al (2013) Cyclin-dependent kinase 1-dependent phosphorylation of cAMP response element-binding protein decreases chromatin occupancy. J Biol Chem 288:23765–23775. doi:10.1074/jbc.M113.464057
29. St-Pierre J, Drori S, Uldry M et al (2006) Suppression of reactive oxygen species and neurodegeneration by the PGC-1 transcriptional coactivators. Cell 127:397–408. doi:10.1016/j.cell.2006.09.024
30. Lee B, Cao R, Choi Y-S et al (2009) The CREB/CRE transcriptional pathway: protection against oxidative stress-mediated neuronal cell death. J Neurochem 108:1251–1265. doi:10.1111/j.1471-4159.2008.05864.x
31. Tan Y-W, Zhang S-J, Hoffmann T, Bading H (2012) Increasing levels of wild-type CREB up-regulates several activity-regulated inhibitor of death (AID) genes and promotes neuronal survival. BMC Neurosci 13:48. doi:10.1186/1471-2202-13-48
32. Mosmann T (1983) Rapid colorimetric assay for cellular growth and survival: application to proliferation and cytotoxicity assays. J Immunol Methods 65:55–63
33. Carcagno AL, Giono LE, Marazita MC et al (2012) E2F1 induces p19INK4d, a protein involved in the DNA damage response, following UV irradiation. Mol Cell Biochem 366:123–129. doi:10.1007/s11010-012-1289-8
34. Ceruti JM, Scassa ME, Fló JM et al (2005) Induction of p19INK4d in response to ultraviolet light improves DNA repair and confers resistance to apoptosis in neuroblastoma cells. Oncogene 24:4065–4080. doi:10.1038/sj.onc.1208570
35. Varone CL, Giono LE, Ochoa A et al (1999) Transcriptional regulation of 5-aminolevulinate synthase by phenobarbital and cAMP-dependent protein kinase. Arch Biochem Biophys 372:261–270. doi:10.1006/abbi.1999.1470
36. Verdeil G, Puthier D, Nguyen C et al (2002) Gene profiling approach to establish the molecular bases for partial versus full activation of naïve CD8 T lymphocytes. Ann N Y Acad Sci 975:68–76
37. Sherman BT, Huang DW, Tan Q et al (2007) DAVID knowledgebase: a gene-centered database integrating heterogeneous gene annotation resources to facilitate high-throughput gene functional analysis. BMC Bioinform 8:426. doi:10.1186/1471-2105-8-426
38. Yamamoto KK, Gonzalez GA, Biggs WH, Montminy MR (1988) Phosphorylation-induced binding and transcriptional efficacy of nuclear factor CREB. Nature 334:494–498. doi:10.1038/334494a0
39. Lee HJ, Mignacca RC, Sakamoto KM (1995) Transcriptional activation of egr-1 by granulocyte-macrophage colony-stimulating factor but not interleukin 3 requires phosphorylation of cAMP response element-binding protein (CREB) on serine 133. J Biol Chem 270:15979–15983
40. Yi C, He C (2013) DNA repair by reversal of DNA damage. Cold Spring Harb Perspect Biol 5:a012575. doi:10.1101/cshperspect.a012575
41. Huang DW, Sherman BT, Tan Q et al (2007) DAVID bioinformatics resources: expanded annotation database and novel algorithms to better extract biology from large gene lists. Nucleic Acids Res 35:W169–W175. doi:10.1093/nar/gkm415

42. Huang DW, Sherman BT, Lempicki RA (2009) Systematic and integrative analysis of large gene lists using DAVID bioinformatics resources. Nat Protoc 4:44–57. doi:10.1038/nprot.2008.211
43. Zou J, Crews F (2006) CREB and NF-kappaB transcription factors regulate sensitivity to excitotoxic and oxidative stress induced neuronal cell death. Cell Mol Neurobiol 26:385–405. doi:10.1007/s10571-006-9045-9
44. Volakakis N, Kadkhodaei B, Joodmardi E et al (2010) NR4A orphan nuclear receptors as mediators of CREB-dependent neuroprotection. Proc Natl Acad Sci USA 107:12317–12322. doi:10.1073/pnas.1007088107
45. Andreoli C, Leopardi P, Rossi S, Crebelli R (1999) Processing of DNA damage induced by hydrogen peroxide and methyl methanesulfonate in human lymphocytes: analysis by alkaline single cell gel electrophoresis and cytogenetic methods. Mutagenesis 14:497–504
46. Mantha AK, Sarkar B, Tell G (2014) A short review on the implications of base excision repair pathway for neurons: relevance to neurodegenerative diseases. Mitochondrion 16:38–49. doi:10.1016/j.mito.2013.10.007
47. Yang J-L, Tadokoro T, Keijzers G et al (2010) Neurons efficiently repair glutamate-induced oxidative DNA damage by a process involving CREB-mediated up-regulation of apurinic endonuclease 1. J Biol Chem 285:28191–28199. doi:10.1074/jbc.M109.082883
48. Li C, Hu Z, Lu J et al (2007) Genetic polymorphisms in DNA base-excision repair genes ADPRT, XRCC1, and APE1 and the risk of squamous cell carcinoma of the head and neck. Cancer 110:867–875. doi:10.1002/cncr.22861
49. Wittschieben BØ, Iwai S, Wood RD (2005) DDB1-DDB2 (xeroderma pigmentosum group E) protein complex recognizes a cyclobutane pyrimidine dimer, mismatches, apurinic/apyrimidinic sites, and compound lesions in DNA. J Biol Chem 280:39982–39989. doi:10.1074/jbc.M507854200
50. Miao F, Bouziane M, Dammann R et al (2000) 3-Methyladenine-DNA glycosylase (MPG protein) interacts with human RAD23 proteins. J Biol Chem 275:28433–28438. doi:10.1074/jbc.M001064200
51. Grombacher T, Mitra S, Kaina B (1996) Induction of the alkyltransferase (MGMT) gene by DNA damaging agents and the glucocorticoid dexamethasone and comparison with the response of base excision repair genes. Carcinogenesis 17:2329–2336
52. Shiyanov P, Nag A, Raychaudhuri P (1999) Cullin 4A associates with the UV-damaged DNA-binding protein DDB. J Biol Chem 274:35309–35312
53. Groisman R, Polanowska J, Kuraoka I et al (2003) The ubiquitin ligase activity in the DDB2 and CSA complexes is differentially regulated by the COP9 signalosome in response to DNA damage. Cell 113:357–367